Problems of Planetology, Cosmochemistry and Meteoritica

Barenbaum A.A. Mechanism of asthenosphere formation on the terrestrial planets

Oil and Gas Research Institute RAS, Moscow

Abstract. Formation on terrestrial planets (Earth, Mars and Venus) asthenosphere is the problem which is not yet received a satisfactory solution. We present the hypothesis according to which the asthenosphere layer is created due to heating lithosphere rocks by shock waves from the galactic comets collapsing in gas shell planets. The paper presents the physical mechanism of the heating and assessment energy of this process. We concluded that asthenosphere is the layer of rocks in base of the lithosphere that is heated to a state of partial melting by capacity to about 200-300 km and moving under planet's surface into the areas with the highest density of fallings galactic comets. The current structure of the asthenosphere Mars and Earth is largely determined by the last bombardment of Solar system by galactic comets in the period from 5 to 1 million years ago.

Keywords: asthenosphere, galactic comets, shock waves, tectonic-magmatic processes, asthenospheric lens.

Barenbaum A.A. (2014). Mechanism of asthenosphere formation on the terrestrial planets. *Experimental geochemistry*. V. 3. N .

http://exp-geochem.ru/JPdf/2015/01/Barenbaum_rus.pdf

Preamble. This article continues the study initiated earlier by the author [Barenbaum, 2002, 2010] on the justification of a new approach to solving problems of the comparative planetary science, based on the accounting of consequences falls of galactic comets on the planets of Solar system. The physical mechanism of the interaction of these comets with Earth is discussed in [Barenbaum, 2012, 2013]. In work [Barenbaum, 2014] on the basis of this mechanism is shown that falling of galactic comets may cause the similar tectonic-magmatic processes on the terrestrial planets which have a gas shell. In present paper, we used this mechanism to explain the sameness of formation and structure asthenosphere on the Earth, Mars and Venus. The emphasis in dealing with this problem is made on the analysis of data for Earth, which studied much better than the other planets.

Problem of asthenosphere emergence. The asthenosphere is called layer rocks of high ductility that underlying a hard cold lithosphere. This layer was open in 1914 after the discovery of phenomenon isostasy. Initially asthenosphere is considered as a continuous geospheric sheath covering the planet as a whole. But today in this shell are installed discontinuities. And therefore the asthenosphere is often seen as a system of overlapping asthenospheric lenses of different size.

The depth and thickness of asthenosphere layer are strongly varied. Under mid-ocean ridges roofing of asthenosphere is at a depth of 2–7 km from the bottom surface. But depth of roofing declines to 80–100 km with removal of ridges on periphery of oceans. Under continents the boundary between lithosphere and asthenosphere lies even lower. Under the ancient platforms, it is located at a depth of 150–200 km, and in South Africa at a depth even of 350 km. However, in the arched parts of young mountain structures, roofing of asthenosphere rises to a depth of 20–25 km. The lower border of asthenosphere is determined less confident. It is assumed that it can reach a depth of 400 km.

According to modern concepts, the asthenosphere layer consists from strongly and unevenly heated rocks of the crust and upper mantle which melting experienced on the level of several first percents. In a result of melting the rocks of asthenosphere have a viscosity of hundreds – thousands of times lower than that for the rocks lying above and below. Due to differences composition minerals of crust and mantle in result melting of the first (at shallow depths) is generated the basaltic magma, and of the second (at great depths) is formed the magma of ultramafic composition. Moving ductile material of asthenosphere, including the formation of the intrusive and extrusive rocks due to cooling of magma induces horizontal and vertical movements of the overlying lithosphere. That is the cause of all planetary tectonic-magmatic and geodynamic processes on Earth's surface.

Origin of asthenospheric layer and features of its structure under the continents and oceans is accepted to associate with the heat flux coming from the Earth's interior. Than this flow is greater, asthenospheric layer is more powerful and it is located closer to the surface.

A controversial in this explanation is the issue of the heat source and the heating mechanism of rocks at depths of ~10÷200 km [Khain, 2003]. According to one hypothesis, the heating is caused by convection in mantle. Hot mantle substance comes from great depths to the surface, where it moves the overlying blocks of cold continental lithosphere. According the other hypothesis, the heating produce hot fluids that in the form of plumes rise to base of lithosphere, where they create melted layer rocks. It is believed that sources of plumes are the processes of differentiation matter on the borders of phase transitions in mantle. Initially it was assumed that the fluids are born on border of lower mantle and Earth core. But now the origin of plumes is explained by similar processes into upper mantle, which has a multilayer structure.

The inadequacy of existing representations manifest themselves in attempts to combine the mantle convection with the phenomenon of intraplate magmatism [Nikishin, 2004], as well as explain the

phenomenon of newest uplifts of continents in the Pliocene–Quaternary time [Artyushkov, 2004, 2012]. To these difficulties, we also add the fact that simultaneously with the newest uplift on Earth happened formation of craters and the rise surface of continental hemisphere on Mars [Barenbaum, 2004]. Large craters have also arisen on Moon and in two of them Tsiolkovsky and Aitken we today observe tectonic-magmatic processes [Barenbaum, Shpekin, 2011, 2013].

The new approach to solving problem. This approach relies on a system of representations [Barenbaum, 2010], according to which at the Galaxy's motion Sun crosses inkjet streams and spiral sleeves our star system. Every once in such periods lasting ~1–5 million years, all planet of Solar system are subjected by bombardments of galactic comets. During one bombardment, number $\sim 10^4$-10^7 galactic comets could fall to Earth. Most often they bombed our planet by the end of Cambrian and Ordovician, as well as in Triassic. The time interval between bombardments was also highly variable. In the Phanerozoic it varied from 19 million years in Late Cambrian, Permian and Neogene to 37 million years in Silurian and Jurassic. Without exception, all the periods of comet bombardments were chosen as the boundaries stratons of Phanerozoic stratigraphic scale.

Last bombing took place in period from ~5 to 0.7 million years ago at boundary of Neogene and Quaternary, when $\sim 10^5$ comets fell to Earth. Their material mainly composed of water ice and other frozen gases with density ~1.0 g/cm^3. Speed movement of galactic comets relative Sun is 450 km/s. Nuclei of comets have diameter of 0.1÷3.5 km, mass of $10^{12} \div 10^{17}$ g and kinetic energy of $10^{20} \div 10^{25}$ J. Total energy of such comets that they brought on Earth is estimated of $\sim 2.5 \times 10^{27}$ J [Barenbaum, 2012].

This value exceeds hundreds of times the energy released totally in Phanerozoic by orogeny – 7.25×10^{18} J/ year [Turcotte, Shubert, 1982], by volcanic activity – 2.4×10^{18} J/year [Sorokhtin, 1974] and by seismic vibrations – 1.05×10^{18} J/year [Gutenberg 1963]. The kinetic energy which galactic comets conveyed to Earth in average for Phanerozoic is comparable with a modern heat flow from depths $\sim 10^{21}$ J/year [Zharkov, 1979]. Calculations [Barenbaum and Jasamanov, 2001, 2003, 2004a; Barenbaum, 2006, 2008, 2009, 2010a, 2011] show that the cyclical fallings galactic comets are able to prick lithospheric plates, create seamounts and hotspots, as well as form a large asthenospheric lens which capable to melt the magma volume required to explain observed trappean effusions.

Proposed by author physical mechanism of heating rocks by galactic comets [Barenbaum, 2012, 2013] allows explaining these tectonic-magmatic phenomena. In accordance with this mechanism in the eras of galactic comets fallings in lithosphere bottom occurs uneven heating layer of rocks with their partially melting of. The formation of this layer, which, strictly speaking, is the asthenosphere, leads by increasing the volume of rock to a significant uplifts surface of continents, and in oceans it causes intense outpouring of lava for bottom, especially in the zones of mid-oceanic ridges.

Mechanism of heating rocks. This mechanism on Earth (and other planets with a gas shell) has the three-step character. At the first stage in the Earth's atmosphere, comet nucleus is transformed into peculiar gas-fluid jet consisting of cometary material subjected to ablation and shock-heated air. In the second stage this jet drops on solid surface, creating narrow-directed hypersonic shock wave which penetrates deep into lithosphere and creates heating of cylindrical column of rocks. The heat effect is so great that rocks in top part of column are vaporized, forming crater. And material under crater is melted, forming an elongated magma chamber. Finally, in the third step, there is a redistribution of heat as in a heated column and in the environment. Time of redistribution heat, depending on comet size and the thermobaric conditions of lithosphere takes $\sim 10^4$-10^6 years [Barenbaum, 2013].

Calculations show that if small galactic comets are able to heat lithosphere beneath continents to depths ~10–20 km and melt rocks in depth range ~1–3 km, for large comets the heating rocks zone reaches depths ~250–300 km, and the melting of rocks occurs at depths ~6÷40 km. Thus, there is a channel through which the magma from asthenosphere is able to flow to surface for a long time.

It is important to note that according this mechanism, most of the kinetic energy of comets is converted into heat, which is involved in heating and melting of rocks in deep layers of lithosphere. At the same time, depending on structure of the lithosphere, the melting are subjected as rocks of crustal and mantle, that is reflected on the composition of magmas and their future behavior. This causes strong convective processes in rocks of asthenospheric layer, initiating various tectonic-magmatic and geodynamic processes on the surface.

Thus, in contrast to the known hypotheses of forming the asthenosphere by heating rocks "from below", this mechanism suggests heating rocks "from above" by shock waves from collapsing galactic comets in gas shell planet. In [Barenbaum, 2013a, 2013b, 2013c] on basis of this mechanism we proposed decisions for number problematic issues of geology associated with formation volcanogenic basalt layer of oceans crust, kimberlitic pipes, as well as phenomenon of intraplate magmatism.

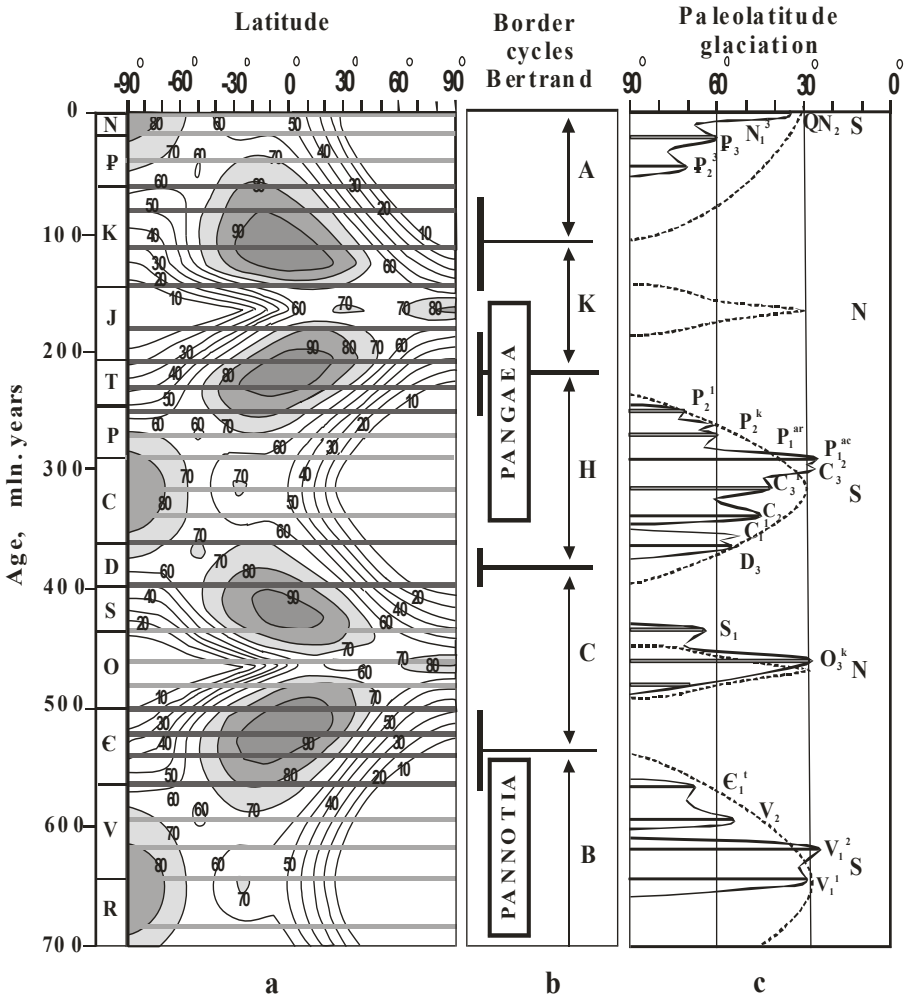

Fig. 1. Comparison of results calculation with actual data: a) density of fallings galactic comets to Earth. The numbers on contour – percentages of maximum intensity. The areas with highest density of falling comets are shown dark color. Narrow horizontal stripes marked periods of cometary bombardments, their duration adopted of 5 million years. In between stripes the calculations are not applicable; b) periods existence of supercontinents Pangea and Pannotia [Bozhko, 2009] and position of boundaries Bertrand's cycles [Chain, 2000]: B – Baikal, C – Caledonian, H – Hercynian, K – Cimmerian, A – Alpine; c) paleolatitudes of spread ice sheets: solid lines – data [Chumakov, 2001], dashed line – calculation [Barenbaum, 2002]. The letters "N" and "S: indicate glaciations caused by bombing of Northern and Southern hemispheres

Theoretical model. This mechanism of heating lithosphere rocks is part of the theoretical model [Barenbaum, 2002], which allows anew to explain of some important geodynamic processes on our and other terrestrial planets. Let us illustrate action of this mechanism on Earth by data on Fig. 1.

Distribution density fallings of galactic comets on breadths of the globe calculated for last 700 million years is shown in Figure 1-a. In the calculation we took into account the Sun movement on galactic orbit, the tilt angle 62º of ecliptic to galactic plane, as well as possible precession of ecliptic with a period of 2.7 ± 0.5 billion years [Barenbaum, Jasamanov, 2004]. In addition, we have adopted to facilitate analysis of calculation results that comets move strictly in the Galaxy plane and their flow does not change for time.

According to our model, frequency fallings of comets reaches maximum at equator and on poles of Earth at certain times. At end of Riphean and in Early Vendian, in Permian-Carboniferous time, as well as in Cenozoic, galactic comets bombed mainly Southern hemisphere of Earth, while most part of Northern hemisphere did not expose their bombing. In Ordovician and Jurassic the pattern was reversed. During these periods, the Sun is in point pericenter of orbit and move with at higher speed. Therefore region of North Pole is subjected to a smaller number of cometary bombarded than the southern. It should be noted that flux of comets bombarded our planet, was greatly mutable. He depended on Sun position in an orbit and dramatically increased when Sun is found in zones starburst of galactic sleeves [Barenbaum, 2010]. Calculations Fig.1 did not take into account these circumstances.

Super-continental cyclicity. Geological data reflecting the cyclical character association of continental blocks into supercontinents on the example of Pangaea and Pannotia [Bozhko, 2009] are shown in Figure 1-b. Taking into account the data on formation and closing of ocean basins in Phanerozoic VE Khain [Khain, 2000] identified the times of increased orogenic activity our planet, which he connected with the boundaries of tectonic cycles by Bertrand and Wilson. Times boundaries Wilson's cycles also shown in Fig. 1-b.

Supercontinents are forming in one of the hemispheres of the planet [Bozhko, 2009]. Following the collapse of one supercontinent on opposite side of globe begins to form another. In this process of continental masses merged together [Condie, 1998] alternately in south and in northern hemisphere. Two major plume events occur during the lifetime of supercontinent: one event during the assembly of the

supercontinent, and the second at end of its existence. The last event is accompanied by continental rifting, introduction of alkaline ultrabasic plutons, outpouring of the basalt with accompanying dolerite dykes as well as diabase and gabbroid sills, which leads to the disintegration of the supercontinent [Khain, 2000]. In recent years the collapse of the supercontinent accepted to connect [Puchkov, 2009] with the action of large igneous provinces – LIPs [Bryan, Ernst, 2008]. These provinces occupy an area more 0.1 million km^2, exist of ~50 million years, and their activity is shown by pulses of ~1-5 million years, during which poured out volume of magma ~10^5-10^6 km^3.

In our model, formation of supercontinents in southern hemisphere in the end of Riphean and Vendian and in Carboniferous is due to lower speed of Sun movement in Galaxy at the aphelion site of its orbit, resulting the southern hemisphere is more often and for a longer time being bombarded by comets, than the north. Alternating excitation of tectonic-magmatic processes in different hemispheres of globe we explain by their alternating bombardments of comets. In result, the boundaries of cycles Bertrand's coincide with the times of most intense falls of comets in the belt widths (-30º, +30º), where density of falling comets reaches a maximum for two – three bombardments. Such picture corresponds quite well to modern views on existence of short-lived LIPs, which show their activity by pulses

Periods of glaciation. Factual data [Chumakov, 2001] about paleolatitudes spread of ice covers for 5 known glacial periods: Laplandian (lower Vendian), border of Vendian – Cambrian, Late Ordovician – Early Silurian, Late Devonian – Early Carboniferous, Middle Carboniferous – Permian (Gondwanian) and late Cenozoic are shown (Fig. 1-c). Last glaciation began in Antarctica in Paleocene and continued in Arctic in Neogene.

Within limits of individual glacial periods is observed alternation of glacial and interglacial phases. The seven such phases were in period of Gondwanian glaciation, at least 4 for Cenozoic, while in periods of Ordovician-Silurian and Laplandian glaciations there were only 2 phases. In our model almost all of glacial phases coincide with times fallings of galactic comets.

The dashed line in Fig. 1 shows the boundary of latitudes above of which in the glacial periods the Earth does not exposed cometary bombardments. We believe [Barenbaum, Jasamanov, 2004] that during of cometary bombardments on Earth's poles, as well as in elevated areas is appeared deposits of ice, that do not have time to melt away between bombardments. An exception must be made for the interglacial phases V1-V2 in Vendian and C1-C2 in Carbon. Note that in these moments, as well as in Late Cretaceous, the Sun is moved on aphelion plot of its orbit at distance of radius corotation from galactic center.

The model easily explains the fact that the border promote ice cover (Fig. 1-b) does not exceed the latitude 30º, as well as allows us to understand the reason why bombings of the southern hemisphere cause glaciation longer than the northern. We can explain and other features of glaciations. So, the more later start of Cenozoic glaciation compared with the calculation can be attributed to the absence the Antarctic continent in the South Pole in period of middle and upper Cretaceous. According to geodynamic reconstructions Antarctica was near this pole only at the end of Cretaceous. In Paleogene its height was probably insufficient for development of global glaciation. A further rapid rise of the continent has led to the fact that in Neogene this glaciation also seized northern hemisphere. Similarly, as well as a relatively low-intensity fallings comets, we may explain why in Jurassic there was Callovian cold snap [Chumakov, 2004] rather than glaciation similar on Ordovician – Silurian.

The coincidence paleolatitudes of spread ice sheets with the area of cometary fallings brings us to the conclusion [Barenbaum, 2012] that formation glaciers due to rising surface of continents, this is such phenomenon as the newest uplift crust [Artyushkov, 1994]. According to our data this phenomenon has been caused by last cometary bombardment.

Phenomenon of newest uplift crust. It is known [Artyushkov, 2012] that in Pliocene-Quaternary time on all continents almost simultaneously happened the lifting surface with amplitudes from 100-200 meters to several kilometers. As a result, there was formed the majority of modern mining buildings, plateaus and other positive forms of relief. Particularly large uplift occurred in Central and South Asia, western North and South America, Eastern and Southern Africa and in East Antarctica. Under many of the mountains occurred a rise of asthenosphere, which is accompanied by modern intensive outpouring of magma.

In his last hypothesis EA Artyushkov [Artyushkov, 2012] the uplift of continents explains increase of thickness asthenosphere beneath continents due to decompression ~100 km layer of mantle lithosphere and of entering into it fluid. The composition and the source of fluid and reason of its almost simultaneous arrival at all continents remain unanswered.

Another problematic issue is connected with conclusion [Summerfield, 2000] that phenomena which are similar on the newest tectonic uplifts have not been happened often on our planet in the Phanerozoic. It is believed that in previous ≥100 million years height of relief surface continents did

not exceed a few hundred meters, reaching about 0.5 km away in their inner parts [Artyushkov, 2012].

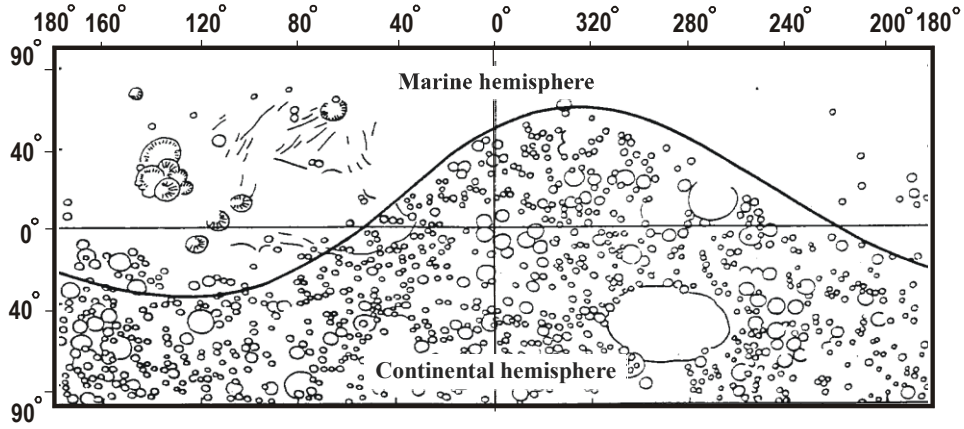

Fig. 2. Structure of Mars surface [Shaded relief map of Mars, 1972]. Curve line is the tectonically border in form of global ledge which separates "marine" and "continental" hemispheres of planet

Our model allows us to look into the matter if we will attract it to analysis of structure topography surface Mars from the positions of comparative planetary [Barenbaum, 2010].

Mars. The axis of rotation Mars, like of Earth, is not strongly deviates from the perpendicular to the ecliptic plane, so the calculations of density cometary fallings (Fig. 1-a) may be applied to Mars. In our model, most important difference between two planets consists in about 100 times less dense of Martian atmosphere than on Earth. Therefore significant part energy of galactic comets is transmitted for formation of large craters. This fact is clearly expressed in topography of Martian surface (Fig. 2).Principal marine and continental forms of surface Mars, as we know, are located on opposite sides of a kind of tectonic boundary obtained in result cutting of spherical surface Mars by plane inclined to its equator at an angle of ~35º [Shevchenko, Rodionova, 1993]. The border is confined to sharp bend relief with a height difference of 2-6 km, which divides Mars like two hemispheres. The differences one from another hemisphere so striking that lets suggest existence of two hemispheres of different ages – "geologically passive" and "geologically active" [Kazimirov, 1977].

Relief of "passive" continental hemisphere is characterized by a large number of craters with a diameter ≥10 km and is identical to continental areas of the Moon. The density of these craters in this hemisphere reaches theoretical limit, which for Mars are ≈100 craters on an area of 10^6 km^2. Craters are distributed exponentially, that pointing to their formation in result of fallings galactic comets [Barenbaum, 2002].

The leading types of relief «active» – marine hemisphere are smooth plains with smooth immersions and uplift of large amplitude [Kazimirov, 1977]. The plains are covered with relatively small craters, density of which is far from saturation. The vast majority of craters have an asteroid's origin. Their diameter distribution obeys inverse-square-law dependence [Voronov et al., 1986]. In equator zone, the plains are crossed of canyons system. Four extinct volcanos in height from 15 to 25 kilometers largest in Solar System are located here.

The nature of surface topography of Mars indicates that formation of its continental hemisphere, similarly to Earth's supercontinents formed in southern hemisphere, is caused by fallings of galactic comets. Their bombardments, especially latter, have created in this hemisphere the thick layer of asthenosphere. To explain difference between the heights of continental and marine hemispheres on Mars, the power of this asthenosphere layer, depending on degree of melting of rocks, should be ~100 ÷ 250 km [Barenbaum, 2004]. At the degree of melting of rocks about 10% emerged magma could easily form on border of mariner hemispheric the system of large volcanoes. It should be noted that our estimate power of layer asthenosphere on Mars coincides well with the power of asthenosphere at the newest uplifts of the continents on Earth [Artyushkov, 2012].

Attraction of information about Mars allows us to refine and complement the theoretical model (Fig. 1-a). Taking into account the daily Mars rotation, the inclination of plane of boundary between its hemispheres in ~35º to the equator of planet gives grounds to assume that in the epoch of falling comets the Mars axis precessed with a period rotation of planet itself. Note that this period is much smaller than the modern period precession of axis Mars constituting estimated ~17.3 thousand years [Solar System, 2008]. It is possible that axis of rotation Earth having precession period today about 26 thousand years, previously experienced something similar.

Another our conclusion is that [Barenbaum, 2002] that at all perturbations of the rotation axis of Mars its northern polar region have not been bombed by galactic comets in last ~60 million years. All the craters with a diameter ≥10 km at the belt latitudes

60º÷90º were created by falling asteroids and comets of Solar system. The distribution of diameters these craters indicate the Cenozoic age of Mars' marine surface [Barenbaum, 2002a].

This result gives us reason to believe that, unlike continental hemisphere that experienced the recent lifting of surface, the "geologically active" marine hemisphere of Mars is in the process of isostatic leveling, which eliminates the previously encountered craters. We assume that the layer of the asthenosphere beneath marine hemisphere of Mars to date is simmer down. Its thickness is decreased and therefore level of marine surface of Mars is lowered. If the speed of this process is the same as on Earth, the period between cometary bombings of ~20-37 million years is quite enough to transform the surface of the marine hemisphere of Mars in low-lying smooth plains.

Since at Sun's movement in Galaxy, galactic comets bombard alternately southern and northern hemisphere of Mars, the asthenosphere layer regularly migrates under the surface of the planet. As a result, through half of Sun's orbital period, marine and continental hemisphere of Mars change places. Judging by super-continental cyclicity (Fig. 1-b), something similar is happening on Earth.

It should be said that cometary bombardments are the main cause of cyclic intensification on Earth mountain-building processes, which received naming orogenic phases Stille. At the same time because of the inertia of heat and mass transfer in layer of asthenosphere the climax Stille's phases usually lag behind from eras of cometary fallings on few million years [Barenbaum et al., 2004].

Data on Earth and Mars are evidence that if in eras of falling comets takes place lifting surface of continents due to heating of rocks asthenosphere layer, while through dozens or hundreds of millions years these rocks experiencing cooling that leads to lowering of continental surface and isostatic compensation of arisen mountain structures. Therefore, the view that the latest orogeny is rarely repeating phenomenon, which was absent in previous more than 100 million years untrue.

In support of conclusion on previously existing on Earth high mountains, which later relatively quickly are leveled, on our opinion, also talks the information about global glaciations (Fig. 1-b).

According to researches of glaciologists [Kotlyakov, 2001] glaciations on Earth can be formed at all latitudes, although at different heights. In equatorial mountainous regions today they are at an altitude of 4 km, which is decreasing to the level of ocean as we approach poles. This conclusion is generic and applicable to the last ice age. Therefore if in the period of cometary bombardment some mainland may prove to be in polar area, uplift of its surface may well be the cause of sheet glaciation.

Good agreement between calculations with actual data gives reason to believe [Barenbaum, 2012] that a necessary condition for development on our planet sheet glaciations is the uplifting of continents similar to newest uplifts. If the amplitude of uplift continents on the pole as at the last cometary bombardment, reaches 1 km or more, this may be enough for appearance in this polar zone glaciation that later may spreading to other parts of planet.

Conclusion

The foregoing materials lead to following conclusions:

1. Availability of the asthenosphere – this is not a purely Earthly phenomenon, but a cosmic phenomenon common to all terrestrial planets. Its cause is a periodic bombardment of Solar system by galactic comets.

2. Heating of rocks lithosphere to form of lenses composing asthenosphere layer occurs under the action of shock waves that generate a galactic comets disintegrating in gaseous envelope of planets.

3. Because of Sun's orbital motion in Galaxy, zone of maximum heating of layer asthenosphere migrates between poles of planets, activating the tectonic and geodynamic processes on corresponding latitudes.

4. Falling of galactic comets initially causes a flatus of continents surface, which then gives way by their lowering and leveling of any mountain structures. These processes take place against backdrop of lateral motion of continental masses, creation new oceanic crust and extensive magmatic outpourings.

References:

1. Artyushkov, E.V. (1994) Newest uplifts of terrestrial crust on continents as consequences lifting of great hot matter masses from mantle, *Doklady Akad. Nauk*, V.336, №5, pp. 680-683.
2. Artyushkov, EV (2012) Pliocene-Quaternary uplift of crust on continents as result of infiltration into lithosphere out of underlying mantle, *Doklady Akad. Nauk*, V.445, №6, pp. 656-662.
3. Barenbaum, A.A. (2002) *Galaxy, Solar system, Earth. Subordinated processes and evolution*, Moscow: GEOS, 393 p. (in Russian).
4. Barenbaum A.A. (2002a) Estimation of tectonic relaxation time of Mars surface using large asteroid craters distribution, *Microsymposium 36 Vernadsky Inst.-Brown Univ. Abstracts*. MS004.
5. Barenbaum, A.A. (2004) On a singularity of asthenosphere Mars, *Electronic Scientific Information Journal "Herald of the Department Earth Sciences RAS"* №1 (22) '2004 URL: http://www.scgis.ru/russian/cp1251/h_dgggms/1-2004/informbul-1/planet-14.pdf (in Russian).
6. Barenbaum, A.A. (2006) Seamounts as field of contemporary magmatism. Cause and mechanism of their formation, *Materials XXXIX Tectonic*

Conference:"Areas of active tectonic-genesis into modern and ancient Earth history", V.1, Moscow: GEOS, pp. 33-37 (in Russian).
7. Barenbaum, A.A. (2008) Processes in Earth's crust and upper mantle: the problems of mountain building and newest uplift crustal, *Materials XIV International Conference:"Interrelation between surface and deep structure of Earth crust"*, Petrozavodsk: Karelian Research Centre RAS, Part 1, pp. 43-47 (in Russian).
8. Barenbaum, A.A. (2009) Tectonic-magmatic processes in oceans and on continents as consequence fallings of galactic comets, *Materials XVIII International Conference on Marine Geology: "Geology of seas and oceans",* Moscow: GEOS, V.5, pp. 205-209 (in Russian).
9. Barenbaum, A.A. (2010) *Galaxycentric paradigm in geology and astronomy,* Moscow: LIBROKOM, 544 p (in Russian).
10. Barenbaum, A.A. (2010a) Trappean magmatism as consequence of heating asthenosphere by shock waves arising at galactic comets destruction in the atmosphere, *Proceedings of XI International Conference:"Physical-chemical and petrophysical researches in the Earth's sciences"*, Moscow, 11-13, Borok, 14 of October, 2010, pp. 44-47.
11. Barenbaum, A.A. (2010b) *Possible formation mechanism of complexes dikes by galactic comets, Materials XLIII Tectonic Conference: "Tectonics and geodynamics of folded belts and platforms Phanerozoic"*, V.1, Moscow: GEOS, pp. 38-42 (in Russian).
12. Barenbaum, A.A. (2011) Tectonic-magmatic processes in oceans and continents as indicators fallings of galactic comets, *Materials International Conference commemorating V.E. Khain: "Modern state of Earth Sciences"*, Moscow: Moscow State University, http://khain 2011.web.ru/, pp. 166-171 (in Russian).
13. Barenbaum, A.A. (2012) On the origin newest uplifts the crust. New formulation of problems global geodynamics, *Uralian Geological Journal*, № 6 (90), pp. 3-26 (in Russian).
14. Barenbaum, A.A. (2013) Possible mechanism of heating lithosphere rocks galactic comets, *Uralian Geological Journal*, № 1(91), pp. 21-39 (in Russian).
15. Barenbaum, A.A. (2013a) Reaction lithosphere on falls of galactic comets (I): origin of volcanic-basaltic layer of oceanic crust, *Proceedings of XIV International Conference:"Physical-chemical and petrophysical researches in the Earth's sciences"*, GEOKHI–IFZ–IEM–IGEM RAS, Moscow, 7-9, Borok, October 10, 2013, Moscow, pp. 31-34 (in Russian).
16. Barenbaum, A.A. (2013b) Reaction lithosphere on falls of galactic comets (II): origin of diamond-bearing kimberlitic pipes, Ibid. pp. 35-38 (in Russian).
17. Barenbaum, A.A. (2013c) Reaction lithosphere on falls of galactic comets (III): intraplate magmatism and its manifestations, Ibid. pp. 39-42 (in Russian).
18. Barenbaum, A.A. (2014). Tectonic-magmatic consequences of fallings of galactic comets on terrestrial planets, *Experimental geochemistry*, *V.2, №1*, http://exp-geochem.ru/JPdf/2014/01/
19. Barenbaum A.A., J.B. Gladenkov, N.A. Yasamanov (2002) Geochronological scale and astronomical time (modern condition of problem), *Stratigraphy. Geological correlation*, *V.10, №2*, pp. 3-14 (in Russian).
20. Barenbaum, A.A., V.E. Khain, N.A. Yasamanov (2004) Large-scale tectonic cycles: analysis from standpoint of galactic concept, *Vestnik MGU, Ser.4, Geology,* №3, pp. 3-16 (in Russian).
21. Barenbaum, A.A., M.I. Shpekin (2011), About age of the lunar surface, *Vestnik Otdelenia nauk o Zemle RAN*, *V.3*, NZ6011, doi:10.2205/2011NZ000141
22. Barenbaum, A.A., M.I. Shpekin (2013), Galactic comet fall as a source of water on the Moon. *Experiment in Geosciences, V.1, №1* URL:http://exp-geochem.ru/html/01_eng_ list.html.
23. Barenbaum, A.A., N.A. Jasamanov (2001) Seamounts, mid-ocean ridges and galactic comet, *7-th Zonenshain International Conference on plate tectonics, October 30-31, 2001. Abstracts,* Moscow: Nauchny Mir, p. 92.
24. Barenbaum, A.A., N.A. Jasamanov (2003) Galactic comets as one of leading factors of tectonic evolution terrestrial planets, *Materials XXXVI Tectonic Conference: "Tectonics and geodynamics continental lithosphere",* V.1. Moscow: GEOS, pp.24-26.
25. Barenbaum, A.A., N.A. Jasamanov (2004) About possible cause of glaciations, *Bulletin of Moscow Society of Naturalists, Dep. Geology, V.79, № 6*, pp. 13-21 (in Russian).
26. Barenbaum, A.A., N.A. Jasamanov (2004a) Tectonic cycles Wilson's, Bertrand and Stille as consequence bombardments Earth by galactic comet, *Materials XXXVII Tectonic Conference: "Evolution of tectonic processes in Earth's history", V.1*, Novosibirsk: SO RAS, pp. 38-41.
27. Bozhko, NA (2009) Super-continental cyclicality in Earth's history, *Vestnik MGU, Ser.4, Geology,* №2, pp.13-28 (in Russian).
28. Voronov, A., R.G. Strom, M. Garkis (1986) Interpretation of annals craters: from Mercury to Ganymede and Callisto, *The moons of Jupiter,* ed. D. Morrison, Moscow: Mir, Part 2, pp. 5-48.
29. Gutenberg, B. (1963) *Physics of Earth's bowels*, Moscow: Publ. of Foreign Literature.
30. Zharkov, V.N. (1983) *Internal structure of Earth and planets*, Moscow: Nauka. 416 p (in Russian).
31. Kazimirov D.A. (1977) Dissymmetry of terrestrial planets and satellites, and the main phases of their development, *Questions of planetary tectonic-genesis,* Proceedings Geological Institute RAS, Issue 1, Moscow, pp. 23-66 (in Russian).
32. Kotlyakov, V.M. (2001) *Selected writings*. Moscow: Nauka, Book 4, 368 p.
33. Nikishin A.M. (2004) In book: *Modern problems Geotectonics and Geodynamics*. Eds.: Lobkovsky L.I., Nikishin A.M., Khain V.E. Moscow: Scientific World, pp. 262-379 (in Russian).
34. Puchkov, V.N. (2009) "The great dispute" about the plumes: who is right after all? *Geotectonics*, №1, pp. 3-22 (in Russian).
35. Sorokhtin, O.G. (1974) *Global evolution of Earth,* Moscow: Nauka, 184 p (in Russian).

36. *Solar System* (2008). Ed. V.G. Surdin, Moscow: FIZMATLIT, 397 p.
37. Khain, V.E. (2000) Large-scale cyclicity in Earth tectonic history and its possible causes, *Geotectonics*, № 6, pp. 3-14 (in Russian).
38. Khain, B.E. (2003) *Main problems of modern geology*, Moscow: Scientific World, 347 p.
39. Chumakov, N.M. (2001) Periodicity of main glacial events and their correlation with Earth's endogenous activity, *Doklady Akad. Nauk*, V.378, №5, pp.656-659.
40. Chumakov, H.M. (2004) Patterns of global climate changes according geological data, *Stratigraphy. Geological Correlation*, V.12, №2, pp.7-32.
41. Shevchenko V.V., J.F. Rodionova (1993) *Globe Mars – yet another "planet" on your desk*, Moscow: Sternberg Astronomical Institute, 28 p.
42. Bryan, S.E., R.E. Ernst (2008) Revised definition of Large Igneous Provinces (LIPs), *Earth-Science Reviews, V.86, №1-4*, pp. 175-202.
43. Condie K.C. (1998) Episodic continental growth and supercontinents: a mantle avalanche connection? *Earth and Planet. Sci. Lett. V.163, № 1-4*, pp. 97-108.
44. *Shaded relief map of Mars* (1972), scale 1:25000000.
45. Summerfield, M.A. (2000) *Geomorphology and Global Tectonics*, N.Y.: Wiley, 386 p.
46. Turcotte, D.L., G. Shubert (1982) *Geodynamics*, N.Y. Yohn Wiley and Sons, V.1-2, 436 p.

Thermodynamic properties of minerals and fluids

Stolyarova T.A., Osadchii E.G., Brichkina E.A. Enthalpy of formation of platinum antimonide $PtSb_2$ from elements

Institute of Experimental Mineralogy RAS, Chernogolovka Moscow district

Abstract. The enthalpy of reaction of formation of platinum antimonide $PtSb_2$ from elements was investigated. The experiments were carried out with high-temperature vacuum-block calorimeter. The synthesis parameters of $PtSb_2$ are in the text. The next value of $PtSb_2$ enthalpy of formation was obtained:

$\Delta_f H^o_{298.15}(PtSb_2, cr)$=-(160.90±1.18) kJ/mol.

Key words: enthalpy, platinum antimonide, geversite, thermochemistry, calorimetry.

Citation: Stolyarova T.A., E.G. Osadchii, E.A. Brichkina. 2015. Enthalpy of formation of platinum antimonide $PtSb_2$ from elements. *Experimental geochemistry*, v. 2, № …

Typical occurrences of platinum antimonide minerals, including geversite, are complex and alluvial platinum deposits. Thermodynamic data of native metals as well as simple binary intermetallic compounds can be used to determine the physical - chemical lower limit of the oxide and chalcogenide mineralization. On the contrary the lack of thermodynamic data makes the physico-chemical analysis of paragenesis (which is the fundamental basis for the understanding of the geochemistry of ore-forming processes) impossible.

Geversite is analogue of mineral sperrylite $PtAs_2$ that has replacement of antimony atoms with arsenic atoms and may have a residual amount of As atoms in the structure (Stumpfle, 1961). In addition, $PtSb_2$ is an extreme member of solid solution series $Pt(Sb,Bi)_2$ (mineral insizvait contains ≥ 50 at.%, (Stefan Schorn and other authors, 1999-2015) in the process of gradual substitution of Sb atoms with Bi atoms, and so may contains an isomorphic admixture of bismuth (Mineral Data Publishing, version 1, 2001-2005). Mineral geversite belongs to the group of pyrite (cubic structure) and has the space group Pa3.

In the study the enthalpy of the next reaction of formation of a binary platinum antimonide was investigated:

$Pt(cr) + 2Sb(cr) = PtSb_2(cr)$

Preliminary investigations showed that $PtSb_2$ synthesis from elements (platinum powder, 99.96 % and stibium powder, 99.99 %) in evacuated quartz glass ampoules took place at 950 °C for 8-10 minutes. The total mass of the sample in each of the nine samples was ~1.8 g.

The calorimetric investigations were carried out with a high-temperature vacuum-block calorimeter, developed in the laboratory of thermodynamics of minerals of IEM RAS, Chernogolovka [Soboleva, Vasil'ev, 1962, Fleisher, Stolyarova, 1978]. A quartz glass ampoule with a sample of given composition was evacuated to a pressure 10^{-4} Torr, sealed and placed into a resistance furnace inside of a calorimetric bomb. The bomb was filled with argon gas under a pressure 10 atm. The isothermal cover of calorimetric bomb was evacuated to residual pressure 10^{-2} Torr. The temperature of the calorimetric isothermal cover (298.15 ±0.02K) was supported automatically with water thermostat of 0.5m^3 volume. Electric energy was measured with accuracy 0.02 %. The temperature increasing during the experiment was measured by a resistance thermometer, consisting of ten miniature cylindrical platinum sensors of temperature, located along the calorimetrical bomb with total resistance 1098 Ohm at 298.15 K. The calorimeter was preliminary calibrated with electric energy in a blank experiment.

The accuracy of thermal value determination is 0.05%. The RMS measurements error was calculated for the 95% confidence interval [Nalimov, 1960]. The results of experiments are placed in the **Table 1.** X-ray powder diffraction analyses of the products confirmed the presence of a given substance only: cubic $PtSb_2$ (geversite) PDF #140141.

As a main result the enthalpy of $PtSb_2$ formation from elements was obtained:

$\Delta_f H^o_{298.15}(PtSb_2, cr) = -(160.90 \pm 1.18)$ kJ/mol.

Table 1. Enthalpy of $PtSb_2$ (geversite) formation from elements (M.M. = 438.58 g/mol)

Number of experiment	Sample weight (g)	ΔR+σ (Ohm)*	The amount of heat released during the experiment (J)			$-\Delta_f H^o_{298.15}$ (kJ/mol)
			total	on the heater	in the reaction	
1	1.7986	12.5676	66819.4	66148.9	670.5	163.50
2	1.8001	12.5130	66529.1	65877.4	651.7	158.78
3	3.2358	12.5976	66978.9	65797.9	1181.0	160.07
4	1.7986	14.0874	74919.6	74257.1	662.5	161.55
5	1.8135	14.0693	74823.3	74158.4	664.9	160.80
6	1.8060	14.1461	75231.8	74563.3	668.5	162.34
7	1.7990	14.1298	75220.0	74563.5	656.5	160.05
8	1.8006	15.6759	83450.6	82790.0	660.6	160.91
9	1.7974	15.6770	83457.1	82800.3	656.8	160.12
The average						160.90 ±1.18

Note:
(*) ΔR+σ – the thermometer resistance value with the correction for thermal exchange,
1-3– samples– calorimeter thermal value W= (5316.8 ±2.0) J/Ohm, 4-6 W= (5318.2 ±2.0) J/Ohm,
7-9 W= (5323.5 ±2.0) J/Ohm.

The study was supported by RFBR grant 12-05-01005.

Authors thank engineers M.V. Fokeev and N.N.Zhdanov for the carrying out the technic part of calorimetric experiments.

References:

1. Fleisher L.L., Stolyarova T.A. 1978. Automating of the process of electric energy measuring in high-temperature calorimeter. *Measuring equipment*. №2. p. 60 (in russian).
2. Nalimov V.V. 1960. Application of mathematical statistics in the analysis of substances. *M. «Nauka»*. 354 p. (in russian).
3. Mineral Data Publishing, version 1. 2001-2005. *http://www.handbookofmineralogy.org/pdfs/geversite.pdf*
4. Soboleva M.S., Vasil'ev Ya. V. The enthalpy of formation of nickel telluride $NiTe_{1.00}$-$NiTe_{1.50}$. 1962. *Vestnik Leningradskogo Universiteta. - Ser. phys. and chem.* v.16. p. 153 (in russian).
5. Stefan Schorn and other authors. 1999-2015. *https://www.mineralienatlas.de/lexikon/index.php/MineralData?mineral=Insizwaite*
6. Stumpfle E.F. 1961. Some new platinoid-rich minerals, identified with the electron microanalyser. *Mineralogical magazine*. Vol.32, №254.

Synthesis of minerals

Martynov[1] K.V., Zakharova[1] E.V., Akhmedjanova[2] G.M., Kotelnikov[2] A.R. Valuation of Cs^+ diffusivities in pore solution of gneiss and dolerite by out-diffusion method

[1]A.N. Frumkin Institutee of Physical Chemistry and Electrochemistry RAS, Moscow
[2]Institute of Experimental Mineralogy RAS, Chernogolovka Moscow district

Abstract. The samples of gneiss and dolerite having density ρ = 2.715 and 3.016 g/cm^3 respectively, made in the form of disks with a diameter of 6.3 cm and 0.7 cm thick, were forcibly impregnated with 0.01 mol/l CsCl solution. After that Cs was leached from pore solution of samples in the distilled water within 140 days at the room temperature. According to various sites of leaching curves reflecting the prevailing processes in different stages of experiment, effective (D_e) and apparent (D_a) diffusion coefficients of Cs^+ were calculated: $4.19 \cdot 10^{-8}$ and $1.57 \cdot 10^{-10}$ cm^2/sec for gneiss and $1.05 \cdot 10^{-7}$ and $1.54 \cdot 10^{-10}$ cm^2/sec for dolerite. Effective coefficients of Cs^+ diffusion in pore solution of rocks correspond in proportion to open porosity (ε) of gneiss (0.0027) and dolerite (0.0071). Coefficients of sorption capacity ($\alpha=D_e/D_a$): 268 and 680, and mass distribution coefficients ($K_d=\alpha/\rho$): 97.5 and 226 cm^3/g for gneiss and dolerite respectively, reflect higher sorption efficiency of dolerite in comparison with gneiss.

Key words: migration of radionuclides, pore diffusion, sorption and diffusive interaction, barrier properties of rocks.

Citation: Martynov, K.V., E.V. Zakharova, G.M. Akhmedjanova, A.R. Kotelnikov. 2015. Valuation of Cs^+ diffusivities in pore solution of gneiss and dolerite by out-diffusion method. *Experimental Geochemistry.* Vol. 3. No. 4. P. X-XX.

http://exp-geochem.ru/JPdf/2015/04/Martynov02_eng.pdf

The main mechanism of radionuclides migration in crystal rocks is advection – transfer of the dissolved, colloidal or pseudo-colloidal species containing radionuclides, by a stream of the underground waters circulating in a massif thanks to a fracture filtration. The factor constraining migration of radionuclides is sorption of species on a surface of rocks minerals. Interaction of fracture

underground waters happens to rock not in all volume of rock, but only on a surface of cracks. And if, except mentioned above, there would be no other factors influencing migration of radionuclides in crystal rock, their barrier properties would be defined generally by the rate of a filtration of underground waters. The contribution of sorption processes on walls of cracks is small as the amount of the radionuclides sorbed in such a way, as a rule, isn't enough owing to insignificance of surface area of cracks even taking into account effect of a roughness. However, the importance of a sorption delay considerably increases due to diffusion of species in pore solution of rocks. Open porosity of crystal rocks is small: from shares to the first units of percent. Therefore the amount of radionuclides which is actually in pore solution as a result of diffusion from fracture water is also negligible. But diffusion makes available to sorption a pore surface which size in specific expression can make to $n \cdot 10^4$ см$^{-1}$. The pore surface provides the sorption capacity of crystal rocks which is one of the main characteristics defining barrier properties of rock massif.

Earlier the model of sorption and diffusive interaction of fracture waters with crystal rocks was offered, the characteristics describing barrier properties of rocks are formulated, and the set of experimental data necessary for calculation of these characteristics is defined [Martynov, 2014]. The model was tested on the example of sorption of Cs and Sr from chloride solutions on gneiss and dolerite – the main rocks composing a massif of the Yeniseiskiy site located close The Mining Chemistry Plant (Krasnoyarsk Krai) and considered for building of object of final HLW isolation. For calculation of barrier characteristics of rocks literary data on diffusivities of Cs and Sr in granites were used. It could increase uncertainty of the received results, especially concerning dolerite, more significantly different from granites on mineral composition and structure than gneiss. For obtaining more reliable data about barrier properties of rocks from the Yeniseiskiy site, the experiments by determination of Cs and Sr diffusion coefficients using the same samples of gneiss and a dolerite were made.

Density (ρ) and open porosity (ε) of rocks examples, determined by water saturation method in accordance to the GOST state standard 26450.1-85, made respectively for gneiss – 2.715 g/cm^3 and 0.0027, for dolerite – 3.016 g/cm^3 and 0.0071. Diffusive experiments were made by out diffusion method. For this purpose the samples of gneiss and dolerite made in the form of disks with a diameter of 6.3 cm and 0.7 cm thick, were forcibly impregnated with water solution of 0.01 mol/l CsCl + 0.01 mol/l $SrCl_2$. Impregnation was made by admission of solution in the container with the samples which are previously dried up at a temperature 120^{o}C to constant weight after its pumping out and endurance under a pressure of 100 Pa within several hours. After that samples were in the sating solution within 2 months for achievement of sorption equilibrium. Then pore solution was leached from samples in the distilled water at the room temperature, with regular agitation within 140 days. Experiments were made in the static mode with periodic replacement by a fresh lot of the leachant (200 cm^3 of water). Further the leachants were acidified by 70% HNO_3, concentrated by evaporation up to the volume of 10 cm^3, and analyzed on the contents of Cs and Sr by emission spectrometry using atomic absorption spectrometer with flame atomizer KORTEK KVANT-2A.

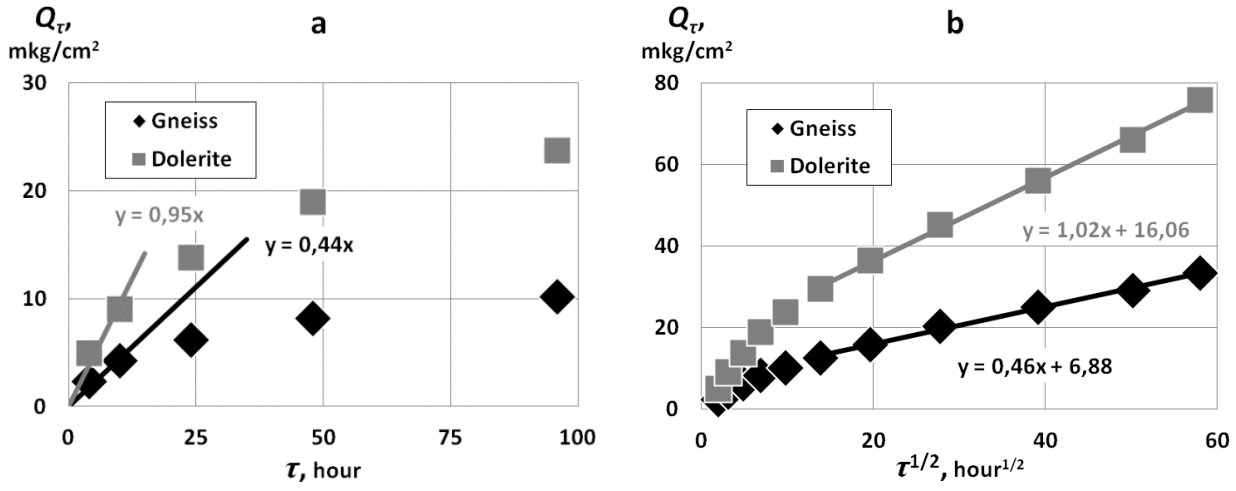

Fig. 1. Curves of Cs leaching from chloride pore solutions of gneiss and dolerite in the distilled water at the room temperature and their approximation lines for the first (a) and the third (b) leaching stages.

The contents of Sr in evaporated leachants were on detection limit of the used analytical method. It is possible to conclude that Sr was practically not leached from pore solution of samples. The explanation of this fact offered by us will be considered below. Results of Cs leaching are presented in fig. 1 as dependences of Cs total quantity leached through 1 cm^2 of sample surface (Q_τ) against the total duration of leaching (τ). Leaching curves can be divided into three sites (stage) corresponding to different processes in a pore space of samples. During the first, the shortest (up to 10 hours) stage, there was a diffusion of Cs^+ from pore solution in leachant at constant maximum concentration of Cs in pore solution (in the central part of a sample) of equal starting concentration, and at constant minimum concentration of Cs in pore solution (in peripheral parts of a sample) of equal equilibrium concentration to sorption saturated pore surface. That is out diffusion at this stage happened in the conditions of full sorption saturation of a pore surface without participation of sorption processes. It allowed to calculate effective coefficients of diffusion:

$$D_e = (Q_\tau \cdot l/2)/(\Delta C_{p.s.} \cdot \tau),$$

where $\Delta C_{p.s.}$ is a difference of starting and sorption equilibrium concentration of Cs in pore solution, l is sample thickness. The relations of Q_τ/τ were defined from experimental data (fig. 1a). Actually, it is tangents to leaching curve at $\tau = 0$. The starting content of Cs in pore solution of samples, equal to its content in the sating solution after achievement of equilibrium, was defined analytically – 934 mkg/cm^3. Concentrations of Cs in pore solution of samples, equilibrium to full sorption saturation of a pore surface, were defined from Langmuir's isotherms of sorption (fig. 2a) and dependences of surface coefficients of distribution (K_A^{ph}) on the contents of Cs in water solutions ($C_{w.s.}$) (fig. 2b), constructed by data [Martynov, 2014] for sorption of Cs from chloride solutions on crushed samples of gneiss and dolerite. Values of Cs sorption equilibrium concentrations in the conditions of sorption saturation of a pore surface were almost negligible: for gneiss – 1.3, for dolerite – 1.1 mkg/cm^3. The calculated sizes of D_e^{Cs+} made for gneiss – $4.19 \cdot 10^{-8}$, for a dolerite – $1.05 \cdot 10^{-7}$ cm^2/sec. Effective coefficients of Cs^+ diffusion in pore solution of rocks correspond in proportion to open porosity of gneiss (0.0027) and dolerite (0.0071).

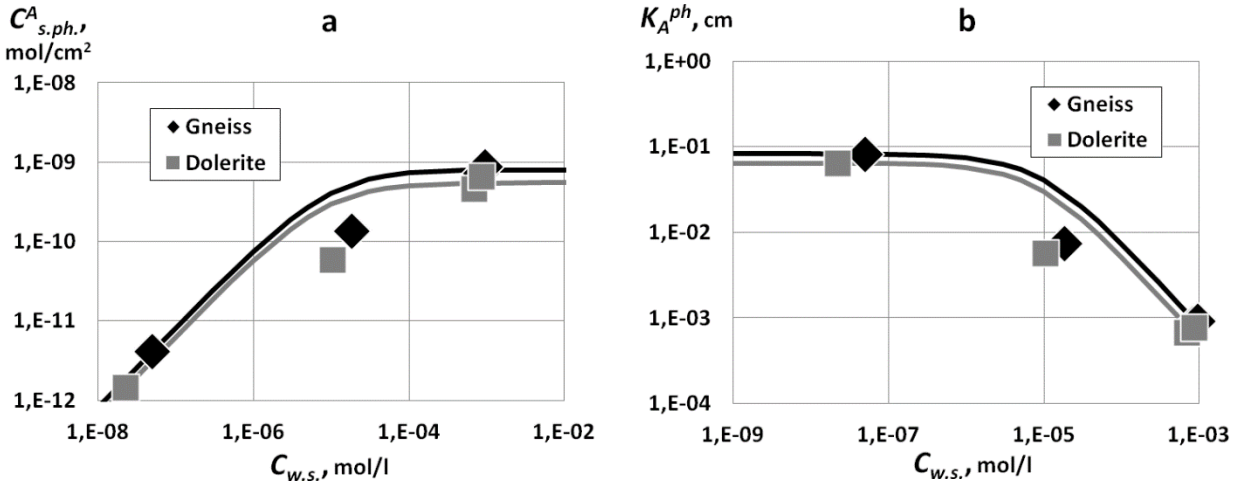

Fig. 2. Langmuir's isotherms of sorption (a) and surface coefficients of distribution (b) for sorption of Cs from chloride solutions on crushed samples of gneiss and dolerite.

At the second stage of leaching there was a change of the maximum concentration of Cs in pore solution from starting to equilibrium with sorption saturated pore surface. Duration of this stage made not less than 4 days (fig. 1). At the third stage process of Cs leaching happened at the maximum concentration of Cs in pore solution equilibrium to sorption saturated pore surface (in the central part of samples) and was followed by Cs desorption from a pore surface and the corresponding reduction of its content in pore solution in peripheral part of samples. Such process can be considered as the return in relation to movement of the diffusive fronts of sorbing species from fracture solution in a porous matrix. Taking into account desorption effect, the apparent diffusion coefficients can be estimated:

$$D_a = Q_\tau^2/[(C^V_{s.ph.})^2 \cdot \tau \cdot \pi].$$

The relations of Q_τ^2/τ are defined from experimental data (fig. 1b). The value $C^V_{s.ph.}$ is a volume contents in samples of Cs sorbed on a pore surface in the conditions of its full saturation:

$$C^V_{s.ph.} = C^A_{s.ph.} \cdot s,$$

where $C^A_{s.ph.}$ is the value of limit sorption saturation of a pore surface of samples which is directly determined by Langmuir's isotherms of sorption (fig. 2a): for gneiss – 0.106, for dolerite – 0.073 mkg/cm^2; s is size of a specific available to sorption pore surface:

$$s = \alpha / K_A^{ph},$$

where α is coefficient of sorption capacity:

$$\alpha = D_e / D_a.$$

Sizes of K_A^{ph} calculated from experimental data (fig. 2b) made for gneiss – 0.082, for dolerite – 0.064 cm. Sizes of s selected so that the ratios given above were carried out. They turned out equal: for gneiss – 3250, and for dolerite – 10590 cm^{-1}. According to these values the apparent coefficients of diffusion D_a^{Cs+} are equal $1.57 \cdot 10^{-10}$ and $1.54 \cdot 10^{-10}$ cm^2/sec, and coefficients of sorption capacity α are equal 268 and 680 for gneiss and dolerite respectively. Mass coefficients of distribution K_d for monolithic samples were calculated from a ratio

$$K_d = \alpha / \rho.$$

They made 97.5 and 226 cm^3/g for gneiss and dolerite respectively.

Table 1. Diffusive and sorption parameters and barrier characteristics of gneiss and dolerite for Cs^+ from chloride solutions

Type of rock	ε	ρ, g/cm^3	D_e, cm^2/sec	D_a, cm^2/sec	K_A^{ph}, cm	s, cm^{-1}	α	K_d, cm^3/g
Gneiss	0.0027	2.715	$4.19 \cdot 10^{-8}$	$1.57 \cdot 10^{-10}$	0.082	3250	268	97.5
Dolerite	0.0071	3.016	$1.05 \cdot 10^{-7}$	$1.54 \cdot 10^{-10}$	0.064	10590	680	226

The calculated diffusive and sorption parameters and barrier characteristics of rocks (tab. 1) reflect higher sorption efficiency of dolerite in comparison with gneiss. The received values of parameters for dolerite quite significantly differ from offered earlier [Martynov, 2014] and, at the same time, are represented more adequate. As an example it is possible to compare new and old values of a specific available to sorption pore surface for a dolerite: 10590 against 90000 cm^{-1}. Really, even for crushed dolerite samples, size of

$$s = a \cdot \rho,$$

where a is the specific surface determined by nitrogen gas adsorption, makes 41100 cm^{-1}. Hardly, it is possible to expect that the monolithic sample will have a size s twice more. On the contrary, the present valuation having about 26% of size for a crushed sample, which should be considered extremely possible, is represented reasonable.

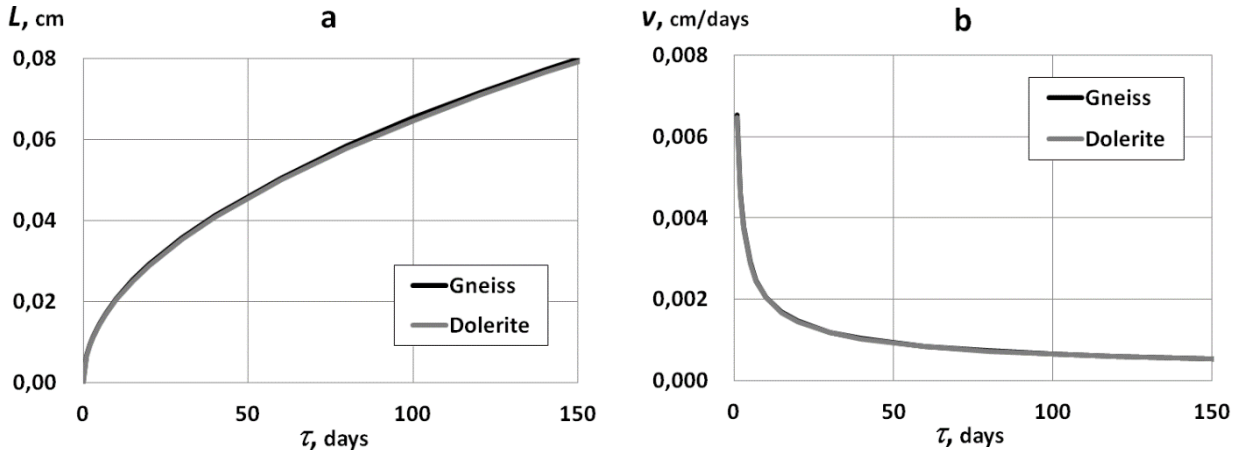

Fig. 3. Depth (a) and rate (b) of Cs^+ diffusive front movement in chloride pore solution of gneiss and dolerite.

It is possible to assume two reasons of emergence of inaccuracies at the previous stage of work. The first which was already mentioned, is using for calculations of inadequate coefficients of diffusion. But there is also other reason: the insufficient duration of sorption experiments with monolithic samples which gave to big errors definitions of experimental parameters against not enough shown effects because of limited time of interaction. So, earlier determined sizes of surface coefficients of distribution for monolithic samples K_A^{geo} made 4.4 and 170 cm for gneiss and a dolerite respectively [Martynov, 2014]. Valuation of sizes K_A^{geo} using parameters from tab. 1, which they are connected with by ratios:

$$K_A^{geo} = K_A^{ph} \cdot L \cdot s = \alpha \cdot L,$$

where L is depth of movement of the diffusive front:

$$L = (\pi \cdot D_a \cdot \tau)^{1/2},$$

gives values for gneiss and dolerite: 6.5 and 16.4 cm respectively. As well as in the previous example, the most essential divergence of values K_A^{geo} is observed for dolerite. Really, during sorption experiments (14 days) on samples of gneiss and a dolerite, depth of the diffusive front for both rocks made 0.25 mm (fig. 3a). It was enough to involve all available to sorption surface of crushed samples (the

size of grains was less than 0.5 mm), but it isn't enough to receive representative results on monolithic samples. Thus rate of movement of the diffusive front

$$v = L/\tau$$

is maximum during initial interval of time (fig. 3b). It increases relative errors of determination of parameters against their small values even more.

Coincidence of depth and rate of Cs^+ diffusive front movement in chloride pore solution for gneiss and dolerite is defined by close values of the apparent diffusion coefficients, and it is sufficiently casual. However it reflects important distinction between effective coefficients of diffusion which ratio is defined mainly by open porosity of rock, and the apparent diffusion coefficients which are inversely proportional a specific available to sorption pore surface:

$$D_a = D_e/(s \cdot K_A^{ph}).$$

We will return to a question of why it wasn't succeeded to observe out diffusion of Sr from pore solution of the studied samples. It is impossible to forget that diffusion is inherent not only to cations, but also anions and neutral species, including water (so-called self-diffusion). Moreover neutral and negatively charged species, as a rule, aren't occluded by rocks and therefore have advantage on diffusion rate before cations. In the case under consideration Cl^- anion was such particle. Its concentration in pore solution decreased quicker, than concentration of cations due to diffusion in the leachant. It didn't affect Cs^+ cation, but Sr^{2+} cation was hydrolyzed and dropped out in a deposit. Thus, change of anion composition of pore solution due to diffusion caused formation of the special hydrochemical barrier which sealed Sr in a pore space of samples. Similar effects at the expense of acid-base, oxidation-reduction and other types of chemical interaction can be observed in actual practice during migration of radionuclides.

Thus, when determining barrier characteristics of crystal rocks in relation to the radionuclides migrating with fracture underground waters it is necessary to pay attention to the following aspects:

1) to use the apparent diffusion coefficients of sorbing species studied on the rocks having structure of porosity similar investigated, or estimated taking into account real sizes of specific available for sorption surface;
2) increase of results reliability requires coordination of the experimental data obtained by different methods;
3) duration of experiments by determination of the parameters connected with diffusion of sorbing species through a low-porous matrix has to be sufficient for receiving reliable data depending on characteristics of a matrix and species;
4) as in the course of experiments, and in actual practice the composition of pore solutions can change at the expense of a combination of diffusive and sorption and chemical interaction.

Reference:

1. Martynov K.V., Konstantinova L.I., Konevnik Yu.V., Zakharova E.V. 2014. Model of sorption and diffusive interaction of solutions flowing in fractures with the low-permeable porous matrix. *Actual problems of radiochemistry and radioecology: Proceedings of the 2nd International Science-Technical Conference.* Ekaterinburg: UrFU. P. 175-180.

Shchekina[1] T.I., Kumanina[1] T.A., Gramenitskiy[1] E.N., Kotelnikov[2] A.P. Experimental study of the solid solution series of Na_3AlF_6–K_3AlF_6 at the temperature of 800^0 and pressure P_{H_2O} =1 kbar

[1]M.V. Lomonosov Moscow State University, Department of Geology, Moscow

[2]Institute of Experimental Mineralogy RAS, Chernogolovka Moscow district

Abstract. In model granite SiO_2-Al_2O_3-Na_2O-K_2O-F-H_2O system at 800^0, 1 kbar all number of phases compositions from Na_3AlF_6 to K_3AlF_6 were received. Its are in equilibrium with the aluminosilicate melts. At the same time only two minerals of this row – purely sodium cryolite Na_3AlF_6 and potassium-sodium elpasolite K_2NaAlF_6. are found naturally. Experiments on their synthesis in hydrothermal conditions at 800^0, 1 kbar were made for studying of this distinction reasons, and also of series compounds of Na_3AlF_6 - K_3AlF_6. properties. The phases received represent a continuous number of compositions from cryolite to elpasolite. The miscibility gap is evident in solid solutions in the range of compositions from the elpasolite to the phase K_3AlF_6.

Keywords: cryolite, elpasolite, solid solution, cryolite similar phase, melt.

Citation: Shchekina T.I.[1], T.A.Kumanina[1], E.N.Gramenitskiy[1], Kotelnikov A.P.[2] Experimental study of the solid solution series of Na_3AlF_6 - K_3AlF_6 at the temperature of 800^0 and pressure P_{H2O} =1 kbar. 2015. *Experimental geochemistry*. V.3. №. Pp.X-XX.

http://exp-geochem.ru/JPdf/201X/XX/XXXXXX_rus.pdf

At high concentration of fluorine in model granite system SiO_2-Al_2O_3-Na_2O-K_2O-F-H_2O there is a crystallization of high-fluorine minerals one of which is the cryolite [Gramenitsky, et al., 2005]. In conditions 800^0, P_{H2O}=1 kbar at various ratios of K/Na in system practically all number of compositions of the cryolite similar phases from Na_3AlF_6 to K_3AlF_6 was received. They are in equilibrium with aluminosilicate melts. In this row clearly inverse correlation of the content of potassium and sodium was observed. Compositions (Na/K relation) of these phases and the coexisting melts are in regular correspondence: sodium collects in solid solution of cryolite, and potassium – in aluminosilicate melt. As a rule, crystals of the

cryolite similar phase crystallized in the melt, were presented by the round or oval segregations from 5 to 30 microns in size and they are homogeneous in composition. Only in some experiments in these crystals were observed lattice structures that were interpreted as signs of decomposition of the solid solution K-Na-cryolite. In rare cases it was possible to estimate the composition of the lamels, characterized by the different ratio of Na/K. At the same time, only two minerals of this series - pure sodium cryolite Na_3AlF_6 and potassium-sodium elpasolite K_2NaAlF_6 are found naturally. Probably one of the reasons for inconsistently between experimental and natural data lies in the lack of knowledge of cryolite composition in granites. On the widely known deposits Ivigtut, Pitinga, Ulugh Tanzek and others within the granite massifs cryolite occurs as disseminated and vein minerals, as well as making up a large body having a commercial value. Experimental results [Gramenitskiy et al., 2005; Alferyeva et al., 2011] point to possibility of the formation of these bodies in the natural conditions of alcalialuminofluoride salt melt in equilibrium with the granite one. These melts were found in the studies of melt inclusions in rare-metal granites and alkaline rocks. Elpasolite is much more rare mineral as compared with cryolite. It occurs in pegmatites of acid and alkaline rocks, as well as in the melt inclusions in quartz and topaz [Pekov et al., 2007]. Potassium cryolite analog K_3AlF_6 is not found in nature, but it is synthesized in dry conditions at the temperatures between 100 and 400^0 C [King et al., 2011]. Information about solid solutions K-Na cryolites (or K-Na hexafluoride, aluminofluoride) in the literature is not found.

The necesity of understanding the properties of the solid solution series Na_3AlF_6–K_3AlF_6 and explaination of the contradiction of experimental and natural data led the authors to the performance of a series of experiments on the synthesis of aluminofluoride Na_3AlF_6 - K_3AlF_6 with aqueous fluid, but without aluminosilicate melt. The material obtained in experiments on the synthesis is under investigation of X-ray and infrared spectroscopy methods. It was not possible to study the properties of these phases in the experiments with melts due to the inability to separate the crystals of aluminofluoride phases from the melt. Complete miscibility in this series aluminofluoride at room temperature was unlikely because phase Na_3AlF_6, K_2NaAlF_6 and K_3AlF_6 have different structures: monoclinic - cryolite, cubic - elpasolit K_2NaAlF_6 [Pekov et al., 2007] and tetragonal - the phase K3AlF6 [King et al., 2011]. However, when the temperature rises cryolite and its potassium analogue undergo phase transitions and have assumed the cubic system: phase Na_3AlF_6 at 560º, and the phase K_3AlF_6 at 400º. This point permits to suggest that at temperatures above 560º can be complete miscibility among Na_3AlF_6–K_3AlF_6 .

The authors performed experiments at 800º, P_{H2O} = 1 kbar, duration of 5-7 days under hydrothermal conditions with the original mixture of compounds Na_3AlF_6 - K_3AlF_6, given by 10 mol.%. In this case, the reagent Na_3AlF_6 and phase K3AlF6 were used. Phase K3AlF6 had previously been specially synthesized in IEM RAS of KF and AlF3 reagents. As liquid phase 10% of KF solution was used. The ratio of the solid charge - the solution is 11: 1. The experiments were performed on a high-pressure equipment in IEM RAS.

The analysis phase was carried out by microprobe complex based on scanning electron microscope «Jeol ISM-6480LV» with a combined system with energy dispersive X-ray microanalysis prefix «INCA-Energy 350" at the Department of Petrology MSU and with the device Camscan MV-2300 of IEM RAS.

The material of experiments was presented typically aggregates intergrown crystals oval or isometric form, sometimes with elements of faceting and the size of the long section of 10 to 800 microns (Fig.1a,b). When the content in the starting mixture was 10-20 (mole%) K_3AlF_6,crystals appear as gomogeneous; with increasing mole fraction of K_3AlF_6 up to 30% the localities composed of a thin (less than 10 micron) symplectitic intergrown phase of two grayscale colors (BSE), appear in them (figure 2 a), which we interpret as indications of decomposition of the solid solution during the rapid quenching.

When the content is about of 70% in the sample, the formation of individual crystals or aggregates of two shades of gray (at BSE) is observed. The a length of crystals is up to 100 and a width up to 30 microns. (Fig. 2 b). In general, the phases have represented a wide range of compositions between the end members of the series Na_3AlF_6–K_3AlF_6. In these as well as in experiments with an aluminosilicate melt, there is a continuous increase of potassium and decrease of sodium minal in synthesized fases, characterized inverse correlation of Na and K (Fig. 3).

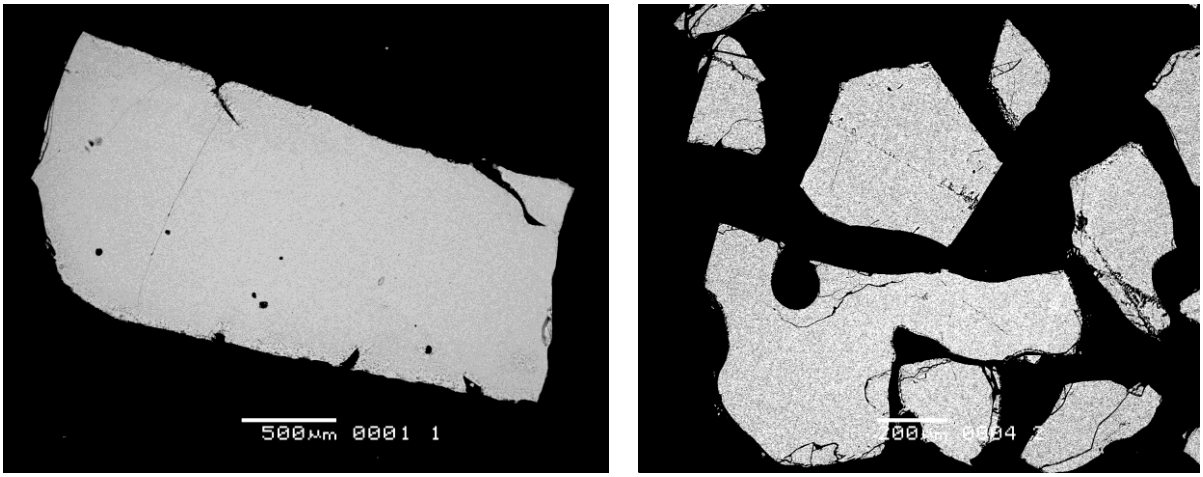

a b

Fig. 1. The form of cryolite similar phases separations in samples of solid solution K_3AlF_6 - K_3AlF_6, comprising: a - 10% K_3AlF_6 (sample 1) - general view of aggregate of small crystals; b - 20% K_3AlF_6 (sample 2) - separations with elements faceting.

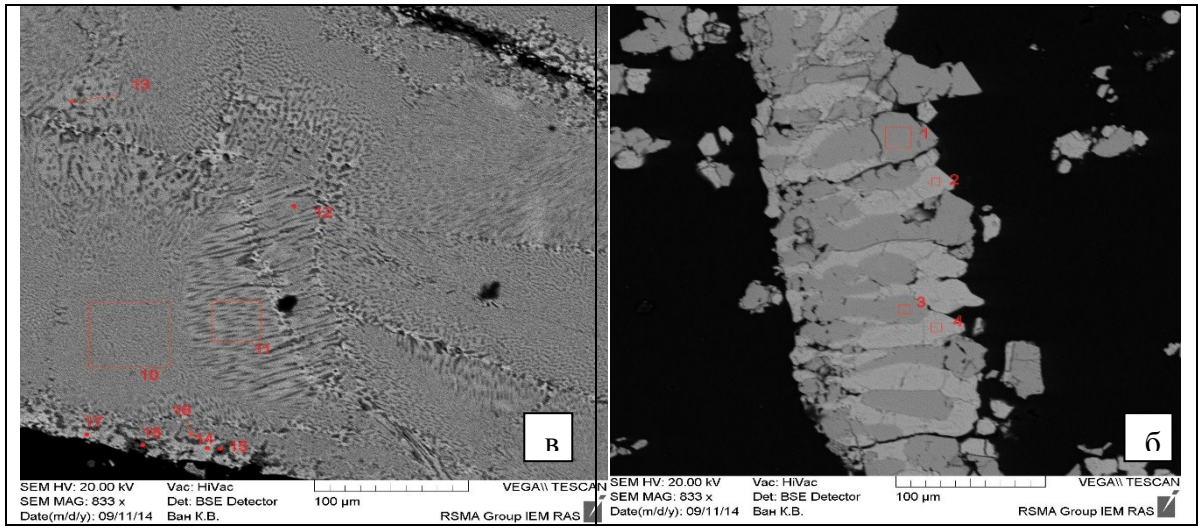

a b

Fig. 2. Structures of exsolution K_3AlF_6- K_3AlF_6: a - quenchening structures in cryolite -elpasolite (sample.3); b - the equilibrium crystal growth with different ratios of Na / K in elpasolite K_2NaAlF_6 - phase K_3AlF_6 (sample 9).

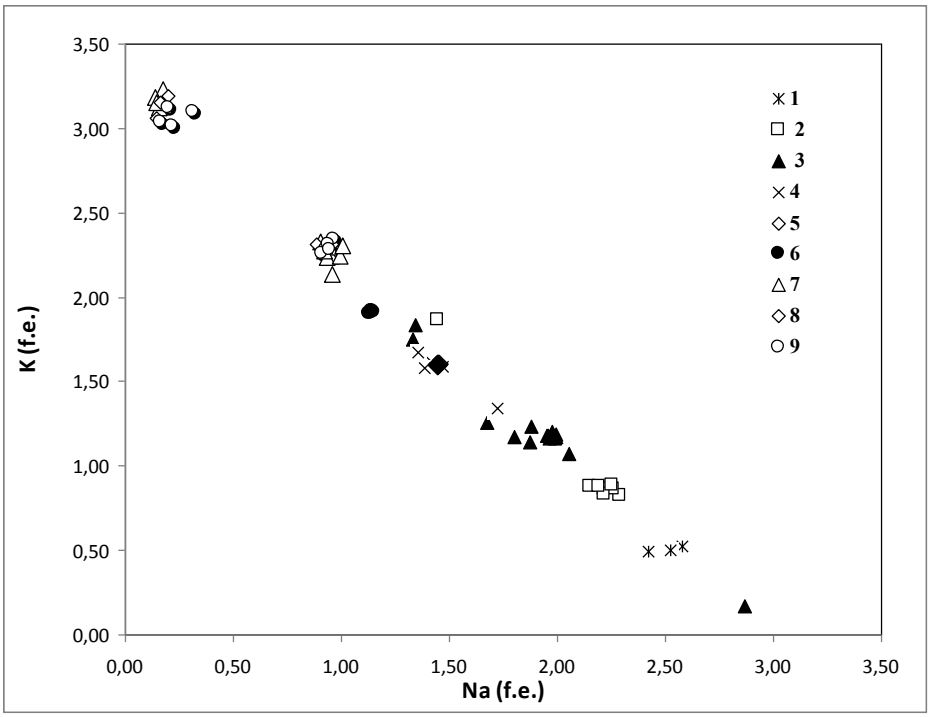

Fig.3. The relation of K и Na (in formula units) in the solid solution Na_3AlF_6- K_3AlF_6. at 800^0 C and P_{H2O} = 1 kbar.

Such character of the solid solution can be regarded as a manifestation of complete miscibility. However in the content of potassium from 2.14 to 3 f.u. there is a gap in the composition of the phases, steadily manifested in three experiments (7, 8, 9), which can be interpreted as a break of solid solution miscibility. The final composition in this proposed area of the immiscibility is closed to K_3AlF_6.and ehlpasolite K_2NaAlF_6. The morphology of the phases in the experiments (Fig. 2 b) confirms this assumption. Phase with smaller and larger content of potassium and sodium minals form reasonable large crystals, have a permanent composition and arose, most likely as a result of co-crystallization. It should be noted that in the area of lower potassium minal content (samples 2, 3, 4) among the crystals constitute the majority were found single phase with more or less ratio of potassium and sodium. In the sample 3 were found smallest intergrowths such phases which are seen as a consequence of the rapid quenching experience. All these doubts authors suggest to solved by X-ray diffraction studies and by the performance of control experiments.

References:

1. Gramenitskiy E.N, Shchekina T.I., Devyatova V.N. 2005. Phase relations in fluorine-containing granite and nepheline syenite systems and distribution of elements between the phases. M.: *GEOS*. 186 p.
2. Alferyeva Y.O, Gramenitskiy E.N, Shchekina T.I. 2011. Experimental study of phase relations in the lithium-rich fluorine gaplogranite and nefelinsyenite system.. *Geochemistry*. 7. Pp. 713-728.
3. Pekov I. V., Chukanov N.D., Kononkova N.N, NV Zubkova N.V, Rabadanov M.K, Pushcharovsky D.Y. 2007. Elpasolite of hyperagpaitic pegmatite in the Khibiny massif (Kola Peninsula). Symmetry of ehlpasolite. *Notes of the Russian Mineralogical Society*. V.307. No 6. Pp. 76-84.
4. King, G., Abakumov, A.M, Woodward P.M, Llobet A., Tsirlin A.A, Batuk D., Antipov E.V. 2011.The High-Temperature Polymorphs of K_3AlF_6. *Inorganic Chemistry*. V. 50. No16. Pp. 7792-7801.

Physical chemical properties of geomaterials

Barenbaum A.A., Klimov D.S. Experimental measurement speed destruction of carbonated water at geosynthesis

Oil and Gas Research Institute RAS, Moscow

Abstract. We presented preliminary results of laboratory experiments to measure speed of destruction of carbonated water in sedimentary cover of Earth's crust under conditions simulating mechanical activation matrix of rocks by action of main natural processes. As an "activator" of rocks we used steel shaving. It is established that degradation rate of water in crustal rocks depends on quantity of dissolved CO_2. In experiments carried out at room temperature this speed was $2.7 \cdot 10^{-5}$g/g H_2O water per hour.

Key words: geo-synthesis of hydrocarbons, carbonated water, activization of matrix rock, hydrogen formation.

Citation: Barenbaum A.A., D.S. Klimov (2015). Experimental measurement speed destruction of carbonated water at geo-synthesis. *Experimental geochemistry*. V. 3. No.

http://exp-geochem.ru/JPdf/2014/01/ Barenbaum & Klimov_rus.pdf

The synthesis of hydrocarbons by the reaction $CO_2 + H_2O$ is a widespread phenomenon of endothermic nature. The energy source in this reaction may be a light (photosynthesis), processes in living organisms (biosynthesis), as well as processes in rocks (geo-synthesis). In the latter case a key role are played underground waters with dissolved in them CO_2 (carbonated water).

In recent years the pumping of carbonated water into productive reservoirs effectively is used to enhance oil recovery factor (ORF) on some oil fields. It is believed that the increase in oil recovery occurs as in result dissolution of inactive hydrocarbons by carbonated water and well by improving mobility of extracted fluid, in general [Ballint, 1977; Alvarado 2010].

Studies show [Zakirov et al., 2013; Semenov et al., 2014] that under certain conditions the carbonated water may decompose to form hydrogen, which together with CO_2 contained in water is capable of participating in the synthesis of hydrocarbons even at room temperature. Possibility of "low temperature" synthesis of hydrocarbons in mineral media (rocks) are water-saturated had been theoretically substantiated and experimentally confirmed in conditions of mechanical activation of carbonaceous rocks previously [Molchanov et al., 1988; Molchanov, Gontsov, 1992; Cherskii, Tsarev, 1984; Cherskii et al., 1985]. In experiments [Molchanov et al., 1988] the activation has been created by crushing and abrasion of solid carbonaceous matter, whereas in experiments [Cherskii et al., 1985] by rotation of models of rocks and by passing water through them.

In conditions of natural occurrence the activization of mineral matrix of rocks may be caused by various natural processes: tectonic, seismic, tidal influence of Moon et al [Cherskii, Tsarev, 1984]. As a result of their action, on the surface of mineral grains are generated radicals [Semenov, 1959], which provide an increment of free energy Gibbs. As a result the threshold reactions of hydrocarbons synthesis, including the reaction $CO_2 + H_2O$, which are thermodynamically allowed at 500-1000º C, on activated surface matrix of rocks begin to take place at room temperature [Cherskii et al., 1985].

According to [Molchanov, Gontsov, 1992], for the low-temperature synthesis of hydrocarbons in rocks of the Earth's crust is necessary to create reducing conditions at which water is able to generate active hydrogen (monatomic or hydride). The same result is known achieved by reacting disperse particles of iron with H_2O. Reacting with water, Fe and its oxides can generate active hydrogen by decomposing water, even at room temperature and atmospheric pressure. This property Fe we used [Zakirov et al., 2013; Semenov et al., 2014] in the study of processes occurring in reservoir bed with carbonated water in conditions of revitalization of matrix rock.

This paper presents the results of laboratory experiments which let to make a preliminary assessment mass of decaying carbonated water in geological environments at the mechanical activated matrix of rocks. We used as "activator" fine crushing iron shavings. The experiments were conducted at a specialized installation in RSU NG them. I.M. Gubkin [Semenov et al., 2014].

Schematic diagram of experiment is shown in Fig. 1.

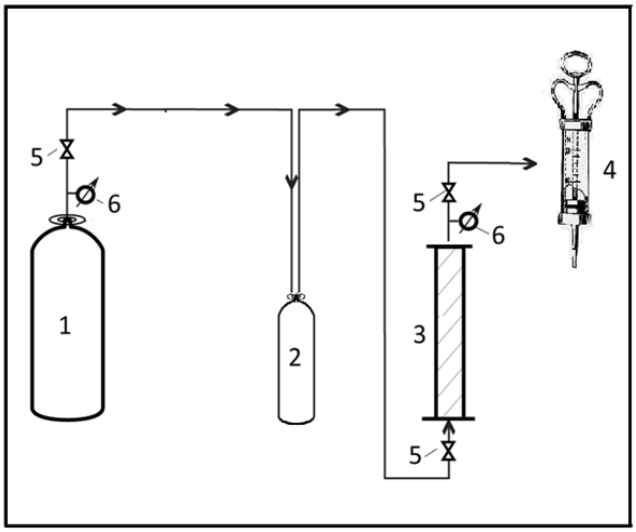

Fig. 1. Schematic diagram of the experiment. Notations: 1 – pressure tank for CO_2; 2 – mixer for making carbonated water; 3 – reactor; 4 – device (measuring syringe), which allows to separate gas phase and to measure its volume; 5 – valves; 6 – Pressure gauges

The reactor represented a cylindrical stainless steel beaker with an internal volume of 45 mL. Into beaker, we loaded 25 g fine shavings of iron (mark ST-3), as well as have lodged carbonated water from mixer under pressure. Volume of water in reactor was 34-36 ml. In the capacity of mixer we used 5 liter container, where the carbonated water was prepared by means saturation of distilled water by chemically purified CO_2 under pressure of 4-5 bar. Before each series of experiments we filled mixer by distilled water on half. Time of water saturation by CO_2 was 18 hours. To separating gas from liquid phase and to measure volume gas at the exit of reactor has been used graduated syringe. Measurement accuracy of gas volume at atmospheric pressure was about ~0.5 cm^3.

The small size of reactor and methodic of measurement were selected based on the results of earlier experiments on a more complex installation with larger volume reactor [Zakirov et al., 2013]. Experiments have shown that when filling of reactor by carbonated water, she is destructed, which eventually leads to an increase in pressure (Fig. 2).

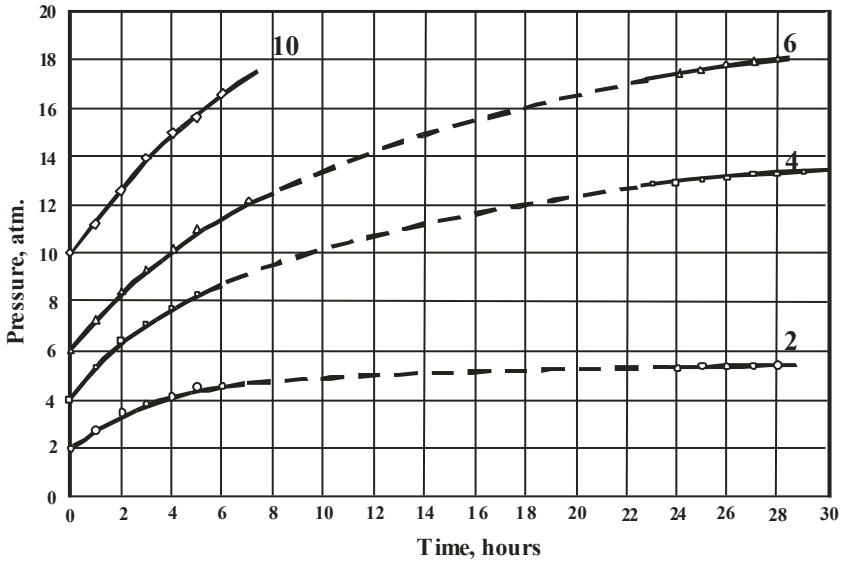

Fig. 2. The time variation of pressure in reactor. Call number curves – initial pressure in reactor after saturation of carbonated water in mixer CO_2

This effect depends on quantity CO_2 dissolved in carbonated water, which may adjusted by means gas pressure and time of cooking water into mixer and may be controlled along value pH of carbonated water.

Gas composition at the reactor outlet after alkaline purification of CO_2 indicates (Table. 1) that the increase in pressure mainly produces hydrogen obtained from H_2O. Nitrogen is supplied from air is contained in water. Oxygen almost completely is trapped by iron, resulting in the ratio of O_2/N_2 becomes lower than in air.

Thus, volume of formed H_2 lets judge on weight of water destroyed in reactor.

Table 1. Chemical composition of gaseous phase after alkali cleaning

Component	Hydrogen	Nitrogen	Oxygen	Methane	Ethane	Propane	Butane	CO_2	CO
Contents %	95.562	3.688	0.657	0.039	0.018	0.0125	0,0049	0,002	0,017

The conclusions of this article are based on 5 measurement cycles volume of gas at several different exposure times. Duration of cycle time is from 3 to 6 days. Experiments were performed at room temperature. Temperature variations in laboratory room during day, as is shown special study, influenced on results of experiments slightly. Therefore special measures for thermostating reactor were not accepted.

In developing methodic we took into account a number of factors that could contribute errors into results of experiment. The first factor was associated with procedure of gas extraction from reactor and determination its volume by syringe, that might lead to ingress of air into measured volume. The second factor was consisted in maintaining constancy of CO_2 saturation in carbonated water before each experiment, that is technically difficult to be controlled, but was required to ensure reproducibility of different series measurements. The third source of error could be due to the fact that after each run we had to wash out reactor and before new measurement again remove air from reactor.

The impact of these factors has been reduced by means special methodic of measurements is illustrated in Fig. 3.

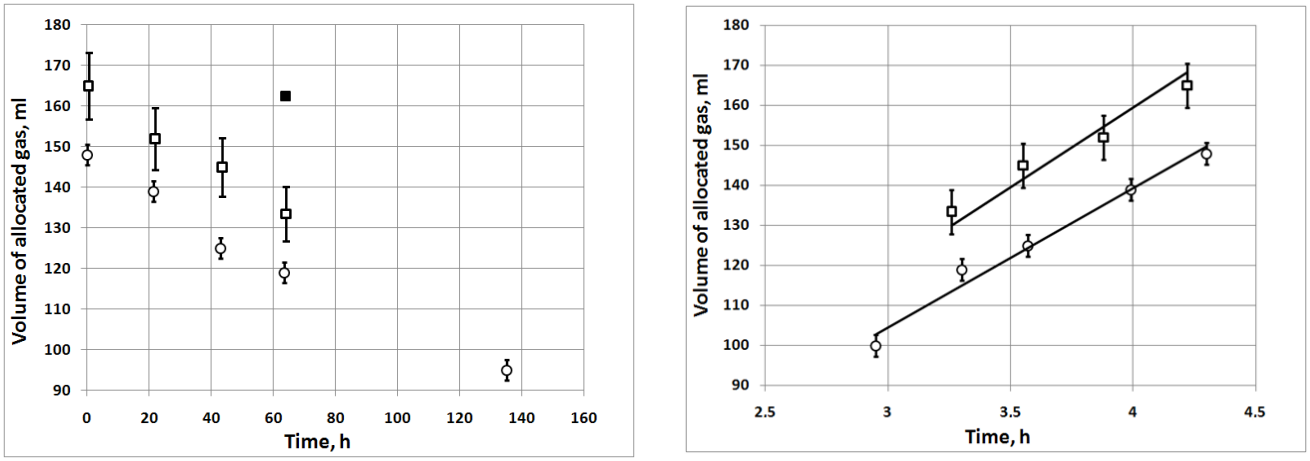

a b

Fig. 3. The volume of evolved gas in depending on: a) time since beginning of experiment, and b) initial pressure of carbonated water in reactor. Mugs – background measurements, squares – informative measurements. Measurement results with exposition of 71 hours are shown with dark square. Straight lines – approximating dependences. Measurement accuracy: background measurements – 2.4% rel., informative measurements – 6.8% rel.

This methodic is in that that during one series of tests, reactor was filled by carbonated water several times, and volume of gas in it was measured after different exposition times (residence time of water in reactor), which we review as "measurements of background" and "informative measurements". Measurements with exposure of 1 minute were considered background. Their gas almost entirely was consisted of CO_2, and its volume corresponded to that, which stands out from the carbonated water after decreasing its pressure from the initial to the atmospheric, where measurements were carried out. Experiments with exposure 21 hours or more were considered informative. In this case along with CO_2 in the gas was presented H_2 which was formed of water. The difference between the informative and background measurements lets to measure amount of formed hydrogen, and through it find amount of water disintegrated in reactor.

With increasing number of measurements, the mass of water and pressure of CO_2 in mixer are decreased with time. The amount of gas, released at depressurization V reactor, is reduced also (Fig. 3-a). The same amount of gas is shown in Fig. 3b in

depending on the initial pressure of gas in the reactor P_o. So how solubility gas is linearly related to the pressure, we approximated dependences V (Po) by straight lines passing through the point P = 0. These dependences have been found by the least squares method and have the form: $V = 34.7\ P_o$ – for background, and $V = 39.0\ P_o$ – for informative experiments. In the latter case, the volume of gas in measurement with exposition of 71 hours has been recalculated on 21 hours as in all other measurements.

Inasmuch as the methodic of sampling gas has been standardized, systematic errors due to possibility of air ingress into system, at transition to difference effect is reduced. The total mean square error determination of volume of hydrogen is 7.2% rel.

Reproducibility of measurement results of two other series of experiments is illustrated in Fig. 4. These cycles are different from the experiments (Fig. 3) by means of replacing of iron's shavings in reactor, the new carbonated water, as well as by sequence of background and informative measurements, that led to the change of approximating dependencies. Those approximating dependencies have the appearance $V = 31.2\ P_o$ for background and $V = 39.2\ P_o$ for informative experiences, at standard deviations of 2.1% rel. and 3.8% rel. respectively.

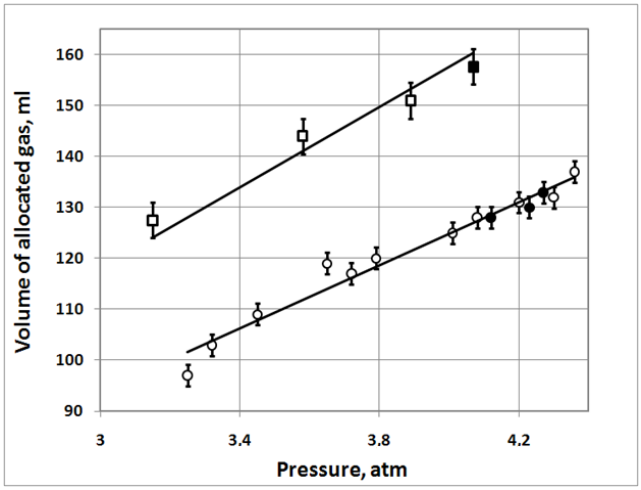

Fig. 4. Comparison of the two series of experiments. Designations as in Fig. 2b. Measurements of second series are shown by dark color. Measurement accuracy: background measurements – 2.1% rel., informative measurements – 3.8% rel.

Comparison of the data in Fig. 3 and Fig. 4 shows that at replacement of carbonated water and shavings the inclination of lines is changed, that affects on difference effect. On "new" shavings (Fig. 4) the effect was 25-28 ml, and at using of shavings that were in the long-term operation the difference effect is reduced to 15-18 ml (Fig. 3).

Averaging results of all experiments, we can adopt that in the limits of 30% rel. in range of initial pressures of 3.0 ÷ 4.3 atm. and time exposition of 21 hours the difference effect is $V_H = 22 \pm 6$ ml. Assuming that the volume V_H completely filled with hydrogen gas, which is at atmospheric pressure has density $\rho_H = 1 \cdot 10^{-4}$ g/cm^3, we obtain amount of generated $M_H = V_H \cdot \rho_H = (2.2 \pm 0.6) \cdot 10^{-3}$ g. Taking into account that proportion of H_2 in water is 11.1%, we find mass of disintegrated water $M = M_H/0.111 = 2.0 \cdot 10^{-2}$ g. Number of disintegrated water, if recalculated on total mass of water in reactor will $M/35 \sim 5.7 \cdot 10^{-4}$. Thus in reactor is disintegrating average $\sim 2.7 \cdot 10^{-5}$ part H_2O in 1 hour.

The issues related with recalculation of experimental results on real sedimentary rocks having considerably greater surface area of matrix than steel shavings and do not containing in their structure a metallic Fe require special investigation.

Authors thank head of department of physical and colloidal chemistry of Gubkin University Oil and Gas of professor V.A. Vinokurov for the opportunity to perform experiments on certificated equipment and employee of this department of A.P. Semenov for help in their conduct.

References:

5. Ballint, V. N. (1977) *Application carbon dioxide in oil extraction*. M.: Nedra, 241 p [In Russian].
6. Alvarado V., E. Manrique (2010) *Enhanced Oil Recovery: Field Planning and Development Strategies.* Gulf Professional Publishing. 208 p.
7. Zakirov S.N., E.S. Zakirov, A.A. Barenbaum, D.S. Klimov, A.D. Lysenko, A.V. Oreshenkov (2013) Nature geosynthesis of hydrocarbons and its consequences, *Proceedings of IV International Scientific Symposium: Theory and practice of enhanced oil recovery methods.* Moscow, VNIIneft. 18-19.10.2013, V.1, pp.130-135 [In Russian].
8. Semenov A.P., E.S. Zakirov, D.S. Klimov (2014) Comparative laboratory studies of processes geo-synthesis on model samples of geological environment, *Technology of oil and gas*. №4 (93), p. 38-44. [In Russian].
9. Molchanov V.I., O.G. Seleznev, E.N. Zhirnov (1988) *Activation of minerals during grinding*. M.: Nedra. 208 p.
10. Molchanov V.I., A.A. Gontsov (1992) *Modeling of oil and gas*. Novosibirsk: OI GMG, 246 p.
11. Cherskii N.V., V.P. Tsarev (1984) Mechanisms synthesis of hydrocarbons from inorganic compounds in upper layers of the crust, *Doklady Academy of Sciences*, V.279, №3. pp. 730-735.
12. Cherskii N.V., V.P. Tsarev, T.I. Soroko, O.L. Kuznetsov (1985) *Influence of tectonic and seismic processes on formation and accumulation of hydrocarbons*. Novosibirsk: Nauka. 224 p.
13. Semenov N.N. (1959) *The main problems of chemical kinetics*. M.: Publ. Academy of Sciences USSR [In Russian].